

## Quantum Sensing with Cavity Optomechanical Array for Gravimetry: Optimization of Entanglement Transfer

Zeynab Faroughi<sup>1</sup> · Ali Ahanj<sup>2</sup>

<sup>1</sup> Faculty of Physics, Shahid Bahonar University of Kerman, Kerman, Iran

<sup>2</sup> Faculty of Science, Department of Physics, Khayyam University, Mashhad, Iran  
email: ahanj@ipm.ir

**Abstract.** Improvement of precision in gravimetry is an important problem in detecting the gravitational waves. In The first demonstration of using quantum, optomechanical cavity in gravimetry has recently been reported. This experiment has been done by employing a cooled levitated nanosphere as a mechanical oscillator in its ground state coupled to a cavity electrodynamics. Following this experiment, in a recent proposal, a quantum optomechanical system has been used for measuring gravitational acceleration. A generic setup for gravimetry purposes, containing two couples optomechanical cavities, where mirrors play the role of oscillating parts. We study such quantum mechanical system, by investigation the dynamics of entanglement between different parts of two coupled cavity optomechanical cells. For such setup, optimal conditions for predesignated entanglement behavior, based on some important parameters of the system, like photon-photon and photon-phonon couplings, electromagnetic field strength and mechanical mode of moving mirrors are analyzed numerically. We show that there exist two different behaviors for entanglement according to selected values for the system parameters.

*Keywords:* Optomechanical cavity , Linear entropy, Mandel's parameter.

## 1 Introduction

Using spatial superpositions of quantum levitated nanoparticles coupled to optical cavities is a new method in acceleration sensing. It is expected that using cavity optomechanical systems improve sensitivity of gravimetry at least 5-orders of magnitude over existing cold-atom sensors [1]. Therefore, such systems will help scientists to develop gravitational wave measurements.

This great development has been made possible by quantum entanglement. Entanglement is one of the most fascinating features of quantum phenomena. Entangled states are important, because of their unique role in quantum information [2]. It is worthy to investigate under which conditions and/or in which systems, entanglement between macroscopic objects is more applicable in technology and applied science [3]. Recent studies clearly show that this goal is achievable in optomechanical systems. Optomechanics is a rapidly developing field of research that explores efficient interactions between photons and mechanical phonons, generally in a quantum electrodynamics (QED) cavity coupled to micro- or nano-scale mechanical objects [4]. Indeed, nano- and micro-mechanical systems are indispensable technologies in modern information age, which enable motional sensing, navigation, timing, and wireless communication [5].

The radiation pressure force is created in the optomechanical cavity due to the momentum carried by light [6, 7]. For the first time, in [8], the authors have shown that the radiation pressure can be used to entangle movable mirrors. In coupled optomechanical cavities, entanglement may be created between different mechanical modes as well as between a cavity mode and a vibration mode.

An important problem (both in theoretical and experimental points of view) is finding the best values for system parameters in order to design the most effective practical setup in the laboratory. What is the behaviour of the system when we choose some values for the system parameters? Coupling the electromagnetic field to the atom, coupling electromagnetic field-mechanical object, strength of electromagnetic field, parameters of mechanical parts, the quality factor of cavity and many more other parameters should be adjusted to find the best desired behaviour in the system. It is not correct that, the maximum values for system parameters are the best values, even for the quality factors. Indeed, system parameters must be adjusted concurrently to achieve desired behaviour. Motivated by this problem, we try to investigate the optimum values of an optomechanical cavity array for the best entanglement transfer between two coupled optomechanical cavities as a gravimeter.

Thus, in the section 2, the theoretical model is introduced by presenting details of the system Hamiltonian. Optomechanical entanglement and its optimal conditions are investigated in the section 3. Conclusions and remarks are presented in the section 4.

## 2 Coupled optomechanical cavities

A cavity optomechanical system is one of the basic elements in acceleration detectors, which can be coupled to each other as shown in figure 1, for using in gravimetry devices [1, 9]. The

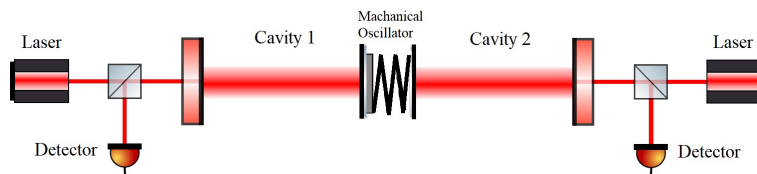


Figure 1: Schematic layout of coupled optomechanical cavities in a quantum network.

standard optomechanical system consists of an optical cavity and a movable mirror. As we study the entanglement transfer between different parts of the system, we have taken two coupled optomechanical cavities, as a typical part of the acceleration detector.

The gravitational interaction between two mirrors is Newtonian picture of quantum mechanics is:

$$\hat{H}_{AB} = -\frac{Gm_A m_B}{|\hat{q}_A - \hat{q}_B|} \quad (1)$$

where  $A$  and  $B$  refers to the movable mechanical mirrors, while  $\hat{q}_A$  and  $\hat{q}_B$  denote quantum operators of their location [9]. Cavity optomechanical Hamiltonian for a movable mirror is:  $\hat{H} = \hbar\Omega\hat{X}\hat{Q}$ , where  $\hat{X}$  is the amplitude quadrature of the cavity mode, and  $\hat{Q}$  denotes for the mirror position  $\hat{q}$  normalized with respect to its zero-point motion. The parameter  $\Omega$  describes the optomechanical coupling strength and the gravitational effect is encoded into this parameter [10].

It is shown that the amount of detectable squeezing is related to the limitations on the quantum radiation pressure in the optomechanical cavities. Such squeezing approximately

is:

$$\mathcal{S} = 2dB \left( \frac{\pi}{\Omega} \right)^4 \left( \frac{Q_m}{3 \times 10^6} \right)^2 \left( \frac{\rho}{20g/cm^3} \right)^2 \quad (2)$$

where  $\rho$  is the material density and  $Q_m$  is the cavity quality factor. As the system is in a steady state, the signal-to-noise ratio increases as the measurement time increases. Thus, we can increase the measurement time  $\tau$  up to a value in which the precision becomes acceptable. Needed measuring time has been calculated as:

$$\tau = 1year \left( \frac{\Omega}{\pi} \right)^3 \left( \frac{3 \times 10^6}{Q_m} \right) \left( \frac{20g/cm^3}{\rho} \right)^2 \quad (3)$$

According to the technology in hand, both  $s$  and  $\tau$  scales are accessible.

We have two coupled cavity optomechanical cells (1 and 2) in gravimetry devices. Thus, the Hamiltonian can be written as [11, 12]:

$$\begin{aligned} H_S = & \omega(a^\dagger a + b^\dagger b) + \Omega/2(c_1^\dagger c_1 + c_2^\dagger c_2) + \lambda(a^\dagger b + b^\dagger a) \\ & -G \left( a^\dagger a(c_1 + c_1^\dagger) + b^\dagger b(c_2 + c_2^\dagger) \right) + H_{AB} \end{aligned} \quad (4)$$

where  $(a, b)$  and  $(c_1, c_2)$  are the annihilation operators of the cavity fields and the mechanical resonators respectively. The coupling strength between two cavities is  $\lambda$ , while  $G$  stands for the coupling strength between photon and phonon fields in the cavity. The parameters  $\omega$  and  $\Omega/2$  are the resonance frequencies related to the electromagnetic energy (photons) and quantized mechanical vibration energy (phonons) of the system. The parameter  $\Omega$  which describes the optomechanical coupling strength is obtained as:

$$\Omega = \sqrt{\frac{2P_{cav}\omega}{m c L \omega_m}} \quad (5)$$

in which  $P_{cav}$  is the intra-cavity optical power,  $\omega$  is the laser frequency,  $m$  is the mirror mass, and  $L$  stands for the cavity length and  $\omega_m$  is the zero point frequency.  $H_{AB}$  is the nontrivial interaction part of the mirror position at the second-order which is:

$$H_{AB} = \hbar \frac{\omega_g^2}{\omega_m} \hat{Q}_A \hat{Q}_B \quad (6)$$

Where  $m = m_A = m_B$  is the mirror masses,  $\omega_g = \sqrt{Gm/d^3}$  and  $d$  is the mean separation of mirrors.

In order to study the dynamics of the system, we have to find time evolution of the system wave function through the Schrodinger equation, or solving the evolution of density matrix using the Heisenberg (or the Lindblad) equation. If we want to study the dissipation and fluctuation terms, we have to arrive at the Heisenberg or Lindblad equations. Here we try to find different behaviours of the system and optimum values for the system parameters, which can be investigated by the wave function. Therefore, we numerically solve the Schrodinger equation for the system. The wave function of the system can be introduced as:

$$|\Psi(t)\rangle = \sum_{a,b,n_{c1},n_{c2}} C_{a,b,n_{c1},n_{c2}} |n_a(t)n_{c1}(t)n_b(t)n_{c2}(t)\rangle = \sum_{a,b,n_1,n_2} C_{a,b,n_1,n_2} |n_a n_1 n_b n_2\rangle \quad (7)$$

where the number of photons in cavities are  $|n_a(t)\rangle$  and  $|n_b(t)\rangle$ , while  $|n_1(t)\rangle$  and  $|n_2(t)\rangle$  stand for number of phonons in cavities. Time evolution of the system wave function is obtained from:

$$i \frac{\partial \Psi(t)}{\partial t} = H_S |\Psi(t)\rangle. \quad (8)$$

Initial state of the system wave function can be considered as:

$$|\Psi(0)\rangle = |n_a(0)n_1(0)n_b(0)n_2(0)\rangle \quad (9)$$

where  $|n_a(0)\rangle$ ,  $|n_b(0)\rangle$ ,  $|n_1(0)\rangle$  and  $|n_2(0)\rangle$  are initial number of photons and phonons in cavities. According to the Hamiltonian (4) and considering initial state (9), we can write:

$$|\Psi(t)\rangle = \sum_{i=0}^{12} C_i |\Psi_i\rangle \quad (10)$$

with:

$$\begin{aligned} |\Psi_0\rangle &= |n_a, n_1, n_b, n_2\rangle \\ |\Psi_1\rangle &= |(n_a + 1), (n_1 - 1), n_b, n_2\rangle \\ |\Psi_2\rangle &= |(n_a + 1), n_1, (n_b - 1), n_2\rangle \\ |\Psi_3\rangle &= |(n_a + 1), n_1, n_b, (n_2 - 1)\rangle \\ |\Psi_4\rangle &= |(n_a - 1), (n_1 + 1), n_b, n_2\rangle \\ |\Psi_5\rangle &= |(n_a - 1), n_1, (n_b + 1), n_2\rangle \\ |\Psi_6\rangle &= |(n_a - 1), n_1, n_b, (n_2 - 1)\rangle \\ |\Psi_7\rangle &= |n_a, (n_1 + 1), (n_b - 1), n_2\rangle \\ |\Psi_8\rangle &= |n_a, (n_1 + 1), n_b, (n_2 - 1)\rangle \\ |\Psi_9\rangle &= |n_a, (n_1 - 1), (n_b + 1), n_2\rangle \\ |\Psi_{10}\rangle &= |n_a, (n_1 - 1), n_b, (n_2 + 1)\rangle \\ |\Psi_{11}\rangle &= |n_a, n_1, (n_b + 1), (n_2 - 1)\rangle \\ |\Psi_{12}\rangle &= |n_a, n_1, (n_b - 1), (n_2 + 1)\rangle \end{aligned} \quad (11)$$

Time evolution of the expansion coefficients are obtained by solving the following coupled differential equations:

$$\begin{aligned} i\dot{C}_0 &= [\omega(n_a + n_b) + \Omega/2(n_1 + n_2)]C_0 - GC_1\sqrt{n_a + 1}\sqrt{n_1} + \lambda C_2\sqrt{(n_a + 1)n_b} \\ &\quad - GC_4\sqrt{n_a(n_1 + 1)} + \lambda C_5\sqrt{n_a(n_b + 1)} - GC_{11}\sqrt{(n_b + 1)n_2} - GC_{12}\sqrt{n_b(n_2 + 1)} \\ i\dot{C}_1 &= -GC_0\sqrt{n_1(n_a + 1)} + [\omega(n_a + n_b + 1) + \Omega/2(n_1 + n_2 - 1)]C_1 + \lambda C_9\sqrt{(n_a + 1)(n_b + 1)} \\ i\dot{C}_2 &= \lambda C_0\sqrt{(n_a + 1)n_b} + [\omega(n_a + n_b) + \Omega/2(n_1 + n_2)]C_2 - GC_3\sqrt{n_b n_2} \\ i\dot{C}_3 &= -GC_2\sqrt{n_b n_2} + [\omega(n_a + n_b + 1) + \Omega/2(n_1 + n_2 - 1)]C_3 - GC_8\sqrt{(n_a + 1)(n_1 + 1)} \\ &\quad + \lambda C_{11}\sqrt{(n_a + 1)(n_b + 1)} \\ i\dot{C}_4 &= -GC_0\sqrt{n_a(n_1 + 1)} + [\omega(n_a + n_b - 1) + \Omega/2(n_1 + n_2 + 1)]C_4 + \lambda C_7\sqrt{n_b n_a} \\ i\dot{C}_5 &= \lambda C_0\sqrt{(n_b + 1)n_a} + [\omega(n_a + n_b) + \Omega/2(n_1 + n_2)]C_5 - GC_6\sqrt{(n_b + 1)(n_2 + 1)} - GC_9\sqrt{n_a n_1} \\ i\dot{C}_6 &= -GC_5\sqrt{(n_b + 1)(n_2 + 1)} + [\omega(n_a + n_b - 1) + \Omega/2(n_1 + n_2 + 1)]C_6 \\ &\quad - GC_{10}\sqrt{n_a n_1} + \lambda C_{12}\sqrt{n_a n_b} \\ i\dot{C}_7 &= -GC_2\sqrt{(n_1 + 1)(n_a + 1)} + \lambda C_4\sqrt{n_a n_b} + [\omega(n_a + n_b - 1) + \Omega/2(n_1 + n_2 + 1)]C_7 \\ &\quad - GC_8\sqrt{n_2 n_b} \\ i\dot{C}_8 &= -GC_3\sqrt{(n_a + 1)(n_b + 1)} - GC_7\sqrt{n_2 n_b} + [\omega(n_a + n_b) + \Omega/2(n_1 + n_2)]C_8 \\ i\dot{C}_9 &= \lambda C_1\sqrt{(n_a + 1)(n_b + 1)} - GC_5\sqrt{n_a n_1} + [\omega(n_a + n_b + 1) + \Omega/2(n_1 + n_2 - 1)]C_9 \end{aligned} \quad (12)$$

$$\begin{aligned}
& -GC_{10}\sqrt{(n_b+1)(n_2+1)} \\
i\dot{C}_{10} = & -GC_6\sqrt{n_a n_1} - GC_9\sqrt{(n_b+1)(n_2+1)} + [\omega(n_a+n_b) + \Omega/2(n_1+n_2)]C_{10} \\
i\dot{C}_{11} = & -GC_0\sqrt{(n_b+1)n_2} + \lambda C_3\sqrt{(n_a+1)n_b} + [\omega(n_a+n_b+1) + \Omega/2(n_1+n_2-1)]C_{11} \\
i\dot{C}_{12} = & -GC_0\sqrt{(n_2+1)n_b} + \lambda C_6\sqrt{n_a n_b} + [\omega(n_a+n_b-1) + \Omega/2(n_1+n_2+1)]C_{12}.
\end{aligned}$$

Above coupled equations clearly show a full quantum connection between all components of the system, through photon-photon and photon-phonon interactions. In order to find a quantitative description, we have to solve the above equations numerically.

To find a better knowledge about the dynamics of the entanglement, we have to study the evolution of probability transfer between different parts of the system, using an entanglement measure, as the linear entropy for a part of the entangled system. In the first step, we need to calculate the density matrix of the system:

$$\rho_{total} = |\Psi\rangle\langle\Psi| = \left(\sum_{i=0}^{12} C_i|\Psi_i\rangle\right)\left(\sum_{j=0}^{12} C_j^\dagger\langle\Psi_j|\right) = \sum_{i=0}^{12} \sum_{j=0}^{12} C_i C_j^\dagger |\Psi_i\rangle\langle\Psi_j|. \quad (13)$$

To reduce needed calculations, we may take partial trace over some parts of the system. As measuring photons in experiments is more easier than the mechanical modes, we trace out mirror vibrations (phonons) in both subsystems to find the reduced density matrix as follows:

$$\begin{aligned}
\rho_p = & (|C_0|^2 + |C_8|^2 + |C_{10}|^2)|n_a n_b\rangle\langle n_a n_b| + |C_2|^2|(n_a+1)(n_b-1)\rangle\langle(n_a+1)(n_b-1)| \\
& + |C_5|^2|(n_a-1)(n_b+1)\rangle\langle(n_a-1)(n_b+1)| + (|C_1|^2 + |C_3|^2)|(n_a+1)n_b\rangle\langle(n_a+1)n_b| \\
& + (|C_9|^2 + |C_{11}|^2)|n_a(n_b+1)\rangle\langle n_a(n_b+1)| + (|C_4|^2 + |C_6|^2)|(n_a-1)n_b\rangle\langle(n_a-1)n_b| \\
& + (|C_7|^2 + |C_{12}|^2)|n_a(n_b-1)\rangle\langle n_a(n_b-1)| + (C_2^* C_5)|(n_a-1)(n_b+1)\rangle\langle(n_a+1)(n_b-1)| \\
& + (C_5^* C_2)|(n_a+1)(n_b-1)\rangle\langle(n_a-1)(n_b+1)| + (C_1^* C_9 + C_3^* C_{11})|(n_b+1)n_a\rangle\langle(n_a+1)n_b| \\
& + (C_9^* C_1 + C_{11}^* C_3)|(n_a+1)n_b\rangle\langle(n_b+1)n_a| + (C_4^* C_7 + C_6^* C_{12})|n_a(n_b-1)\rangle\langle n_b(n_a-1)| \\
& + (C_7^* C_4 + C_{12}^* C_6)|(n_a-1)n_b\rangle\langle(n_b-1)n_a| \quad (14)
\end{aligned}$$

Now, we need an entanglement measure to study the dynamics of entanglement. The Linear entropy is a suitable criterion which gives the amount of entanglement for the system. In particular, we want to calculate the dynamics of entanglement between the mechanical parts. The higher (lower) entropy, implies the greater (smaller) degree of entanglement. Thus, we are reasonably interested in the calculation of the time evolution of linear entropy of the system. This quantity for moving mirrors reads as  $S_p(t) = 1 - \text{Tr}\rho_p^2(t)$  which is:

$$\begin{aligned}
S_p(t) = & 1 - (|C_0|^2 + |C_8|^2 + |C_{10}|^2)^2 - (|C_1|^2 + |C_3|^2)^2 - (|C_9|^2 + |C_{11}|^2)^2 \\
& - (|C_4|^2 + |C_6|^2)^2 - (|C_7|^2 + |C_{12}|^2)^2 - 2|C_4^* C_7 + C_6^* C_{12}|^2 \\
& - 2|C_1^* C_9 + C_3^* C_{11}|^2 - |C_5|^4 - 2|C_2|^2|C_5|^2 - |C_2|^4 \quad (15)
\end{aligned}$$

If  $S_p = 0$ , subsystem states are totally separable, while there exist some degrees of entanglement between parts of subsystems in the case  $S_m > 0$ .

Another important characteristic for the photon (phonon) statistics of the quantized oscillation is the Mandel's Q parameter which is defined as follows [13]:

$$Q_i = \frac{\langle n_i^2 \rangle - \langle n_i \rangle^2}{\langle n_i \rangle} - 1 \quad (16)$$

in which  $i$  stands for the mechanical modes  $c_1$  and  $c_2$  or for photon numbers  $a$  and  $b$ . The quantum statistics of subsystem  $i$  is sub-Poissonian if  $Q < 0$  which is a non-classical state. For values  $Q = 0$  and  $Q > 0$  subsystem is Poissonian and super-Poissonian statistics, respectively. The  $Q$ -value can be calculated easily through the density matrix (14).

Now, we have two different robust measuring tools for evaluating the dynamics of entanglement. We can pay attention to the problem of optimization of the system parameters for the best performance of an intended feature in the system which can be occurred by the entanglement dynamics.

### 3 The entanglement dynamics

There are several environmental parameters in our system. The most important parameters are photon-photon fields coupling  $\lambda$  and photon-phonon coupling  $G$ . Figure 2 demonstrates time evolution of linear entropy ( $S$ ) and the Mandel's parameter ( $Q$ ) for different values of coupling parameters. This figure clearly shows that two distinct behaviours may occur according to selected values for system parameters, especially couplings  $G$  and  $\lambda$ . The periodic transition of energy between electromagnetic fields of cavities and mechanical vibration of moving mirrors can be established with balanced values of coupling parameters. Periodic evolution of linear entropy (as well as the Mandel parameter  $Q$ ) occurs when  $G > \lambda$ . This means that, if photon-phonon coupling ( $G$ ) becomes larger than the electromagnetic coupling between subsystems ( $\lambda$ ), we expect to find a bidirectional information transfer between subsystems. It may be noted that, for larger values of  $G$ , amplitude of oscillations decreases. Figure 2 shows that amplitude of oscillations for  $\lambda = 0.7$  and  $G = 0.72$  is greater than that for  $G = 1.0$  with the same value for the  $\lambda$ . Our numerical calculations show that for  $G < 0.67$ ,  $S$  and  $Q$  monotonically go toward a fixed value which depends on the other system parameters. It may be noted that the  $Q$  value are always negative, which demonstrates the quantum nature of the system statistics. According to figure 2 one can find that the linear entropy  $S$  is more sensitive measure than the  $Q$  value. Please see the amplitude of oscillations  $S$  and  $Q$  as the parameter  $G$  is changed. The amplitude of Oscillation in the linear entropy is greater than that for the Mandel's parameter  $Q$ .

Figure 3 shows the same plots as figure 2 but with  $\lambda = 0.5$ . Comparing figures 2 and 3 indicates that, entanglement transfer between the system parts is strongly damped with smaller values of coupling coefficient for electromagnetic part (low quality cavities and/or weak cavity coupling). So, according to the required application, we can design the system in oscillating or damping situations. For larger (smaller) entanglement, we can design the system in larger (smaller) photon-phonon and photon-photon couplings, by considering this issue that larger coupling leads the system toward the oscillating regime. We have numerically found the maximum linear entropy  $S$  for different values of system parameters which results have appeared in figure 4. In each plot for a specified value of  $\lambda$ , the linear entropy is constant (respect to time) for values of  $G$  within the increasing part of the curve, while it is oscillating for decreasing part of the plot. As an example, for the  $\lambda = 0.70$ , the maximum value of the  $S$  occurs with  $G = 0.70$ . The profile of linear entropy for  $G = 0.72$  is oscillatory while we have a monotonic curve with  $G = 0.67$ . It should be indicated that, there is not a sharp separation point for these two behaviours and it is better to speak about two overlapping regions.

The entanglement is transferred between different parts of the system by photons. Figure 5 demonstrates the effects of electromagnetic field strength (indeed number of photons) on the time evolution of the entanglement. It is clear that, in the absence of photons, entanglement transfer by the vacuum energy is very small. On the other hand, strong

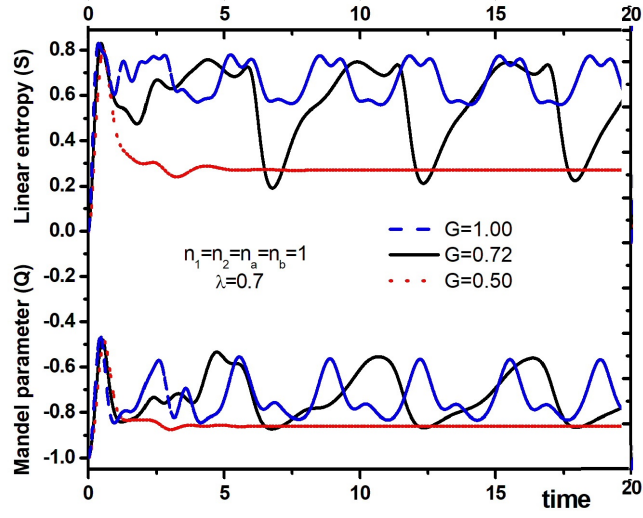


Figure 2: Time evolution of linear entropy  $S$  and Mandel's parameter  $Q$  for different values of  $G$  with  $n_a = n_b = n_1 = n_2 = 1$  and  $\lambda = 0.7$ .

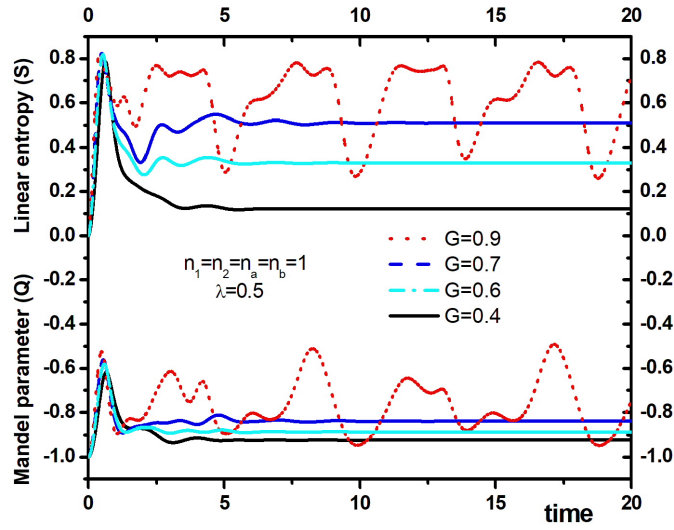


Figure 3: Time evolution of linear entropy  $S$  and Mandel's parameter  $Q$  for different values of  $G$  with  $n_a = n_b = n_1 = n_2 = 1$  and  $\lambda = 0.5$ .

electromagnetic field (i.e. large number of photons) critically change quantum effects in the system, as we can find from figure 5. Comparing the behaviour of linear entropy (and the Mandel's parameter) for  $n_a = 1$  and  $n_a = 2$  (for example) shows that creating a requested behaviour in the system is possible through fine tuning of couplings  $\lambda$  and  $G$  together with the suitable strength of electromagnetic fields in both cavities. Indeed, our numerical calculations show that, the same behaviour is observed for the number of photons in the other cavity ( $n_b$ ).

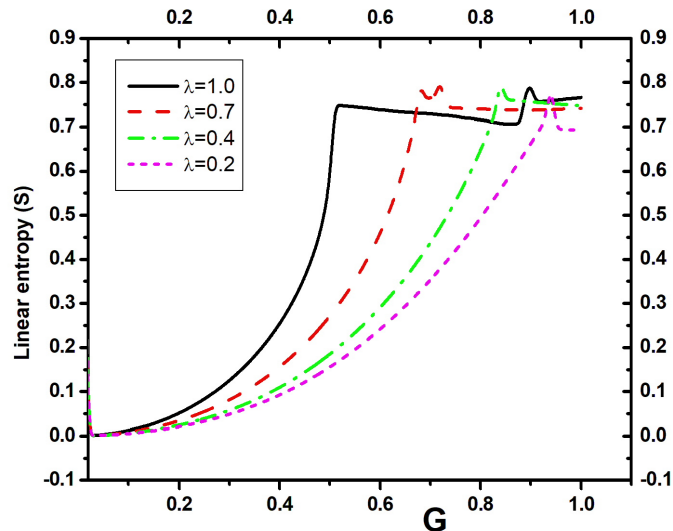


Figure 4: Maximum linear entropy  $S$  for different values of photon-photon and photon-phonon couplings with  $n_1 = n_2 = n_a = n_b = 1$ .

As the final comment, it is interesting to look at the variation of maximum linear entropy as functions of coupling  $\lambda$ . Figure 6 presents the maximum entropy respect to coupling  $\lambda$  with  $n_1 = n_2 = n_a = n_b = 1$  and different values of coupling  $G$ . This figure indicates that, the maximum entropy in all cases can be obtained with maximum accessible value of coupling  $G$ , but not necessarily with maximum value of  $\lambda$ . Indeed, coupling  $\lambda$  should be taken by considering the strength of electromagnetic fields and also mechanical vibration modes in the system.

## 4 Conclusion and Remarks

Dynamical evolution and entanglement exchange in optomechanical parts of a quantum gravimetry setup have been studied. The effects of system parameters: photon-photon coupling, photon-phonon coupling, electromagnetic field strength, and mechanical vibration modes, on the behaviour of entanglement in the system have been investigated, using linear entropy and Mandel's parameter. We have found that two different trajectories can be appeared in the time evolution of entanglement, respect to have taken the values of system parameters. Entanglement may oscillate between electromagnetic and mechanical modes of the system, or it is possible that entanglement monotonically transfers into the mechanical



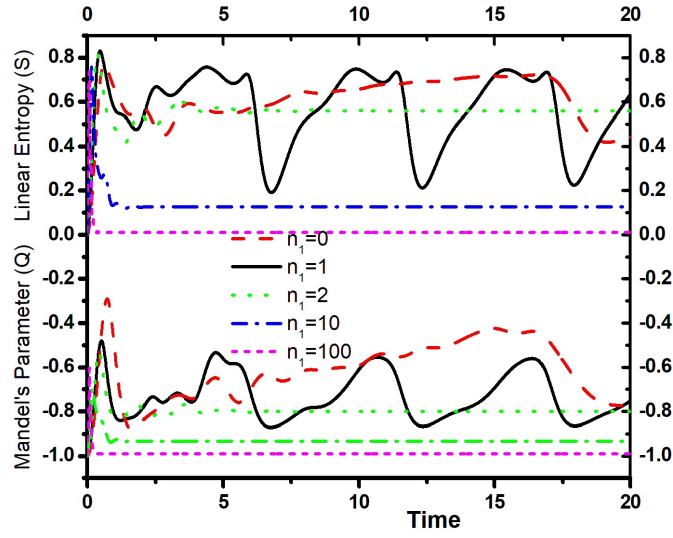


Figure 5: Time evolution of linear entropy  $S$  and Mandel's parameter  $Q$  for different values of electromagnetic field in cavity 1 ( $n_a$ ) with  $n_b = n_1 = n_2 = 1$ ,  $\lambda = 0.7$  and  $G = 0.72$ .

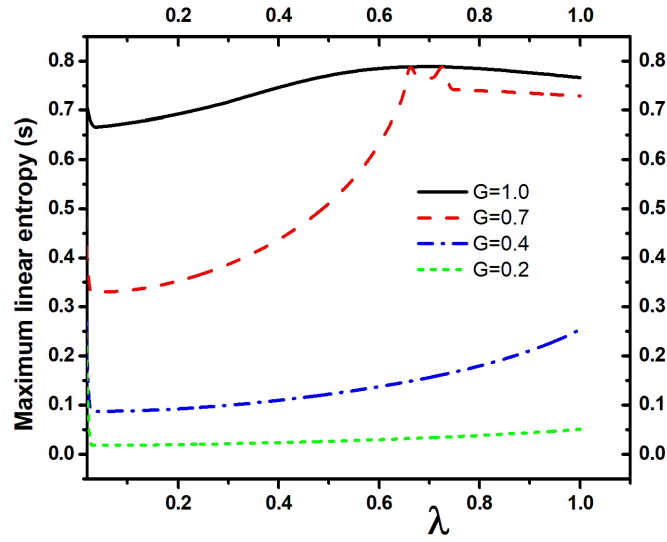


Figure 6: Linear entropy  $S$  as functions of  $\lambda$  with different values of  $G$ . Initial values for photons and phonons are  $n_1 = n_2 = n_a = n_b = 1$ .

modes and the system goes to a stationary state. Both situations can be used in a quantum system, according to the considered role for the optomechanical part in the network. For a typical initial condition, we numerically calculated the maximum linear entropy (and Mandel's parameter) for different values of system parameters. We found that, for the maximum attainable value of photon-photon coupling (cavity quality) and field strength, there exists an optimal value for photon-phonon coupling, which is not necessarily its maximum. We have studied the effects of electromagnetic field strength and also mechanical modes on the quality of information swapping, its maximum value and the dynamical evolution of quantum entanglement. It is shown that quantum properties of the system disappears if the electromagnetic field (number of photons) is too large. However, in the absence of the electromagnetic field in the cavity, quantum properties are also weak.

There are several complementary investigations that should be done. We have not considered dissipative effects in our system. Due to technical limitations, disorders and disruptive in the system play crucial role and therefore, we have to consider such issues to find the actual behaviour of the system. We have not considered feedback effects which may happen in quantum networks. We have not included the non-Markovian process and related dynamics of the equation of motion, which can be considered to find more accurate entanglement measures. These problems can be investigated in further works.

## References

- [1] Rademacher, M., Millen, J., & Lia Li, Y. 2020, *Adv. Opt. Techn.* 2020; aop, DOI: 10.1515/aot-2020-0019
- [2] Paternostro, N., Vitali, D., Gigan, S., Kim, M. S., Brukner, C., Eisert, J., Aspelmeyer, M. 2007, *Phys. Rev. Lett.*, 99, 250401.
- [3] Pinard, M., Dantan, A., Vitali, D., Arcizet, O., Briant, T., Heidmann, A. 2005, *Europhysics Letters*, 72, 747.
- [4] Akram, P., Munro, U., Nemoto, W., Milburn, K., 2019, *Phys. Rev.*, A86, 042306.
- [5] Pennek, D. Y., & Djafari-Rouhani, B. 2019, *Phys. Rev. Applied*, 12, 024002.
- [6] Aspelmeyer, M., Kippenberg, T., Marquardt, F. 2014, *Rev. Mod. Phys.*, 86, 1391.
- [7] Marquardt, F., Harris, J. G. E., & Girvin, S. M. 2006, *Phys. Rev. Lett.*, 96, 103901.
- [8] Mancini, S., Giovannetti, V., Vitali, D., Tombesi, P. 2002, *Phys. Rev. Lett.*, 88, 120401.
- [9] Martynov, H. D., Yang, H., Datta, A. 2020, *Phys. Rev. A*, 101, 063804, DOI: 10.1103/PhysRevA.101.063804
- [10] Metcalfe, M. 2014, *Appl. Phys. Rev.*, 1, 031105
- [11] Law, C. K. 1994, *Phys. Rev.*, A49, 433.
- [12] Law, C. K. 1995, *Phys. Rev.*, A51, 2537.
- [13] Mandel, L, 1979, *Opt. Lett.*, 4, 205.